

MIT Open Access Articles

Impulse breakdown delay in liquid dielectrics

The MIT Faculty has made this article openly available. **Please share** how this access benefits you. Your story matters.

Citation: Jadidian, Jouya, Markus Zahn, Nils Lavesson, Ola Widlund, and Karl Borg. Impulse Breakdown Delay in Liquid Dielectrics. Applied Physics Letters 100, no. 19 (2012): 192910.

As Published: <http://dx.doi.org/10.1063/1.4716464>

Publisher: American Institute of Physics

Persistent URL: <http://hdl.handle.net/1721.1/79377>

Version: Original manuscript: author's manuscript prior to formal peer review

Terms of use: Creative Commons Attribution-Noncommercial-Share Alike 3.0



Impulse breakdown delay in liquid dielectrics

Jouya Jadidian^{1,a)}, Markus Zahn¹, Nils Lavesson², Ola Widlund² and Karl Borg²

¹ *Department of Electrical Engineering and Computer Science, Massachusetts Institute of Technology, MA 02139, USA*

² *ABB Corporate Research, Västerås, SE 72178, Sweden*

Theoretical images of streamers, revealing the mechanisms behind impulse breakdown in liquid dielectrics, are presented. Streamers form paths that are capable of carrying large current amplitudes through the electrode gap, leading to electrical breakdown. Breakdown delays are calculated for different electrode geometries (40 μm needle and 6.35 mm sphere) and gap distances (up to 10 mm) as well as time dependent currents through the gap. Modeling results indicate that the breakdown within needle-needle electrodes requires higher impulse voltage magnitudes than within needle-sphere electrodes for the same gap distances. Streamers in needle-sphere geometries are about 50 percent thicker than streamers propagating in needle-needle geometries under similar impulse voltage amplitudes. [<http://dx.doi.org/10.1063/1.4716464>]

A three-carrier continuum model¹ is utilized to account for the charge generation, recombination and transport mechanisms, which are critical in the study of streamers emanating from a needle electrode, with 40 μm radius of curvature, propagating through a transformer oil based liquid dielectric volume and eventually reaching either grounded needle electrode (with the same radius of curvature) or sphere grounded electrode, with 6.35 mm radii of curvature. The governing equations that contain the physics to model streamer development are based on drift-dominated charge continuity equations for positive ion, negative ion and electron charge densities, coupled through Gauss' law. The thermal diffusion equation is included to model temperature variations and gas formation in oil.^{2,3} The mobility dependencies on electric field intensity⁴ (due to electron velocity saturation at extremely high electric fields) and temperature (due to lower viscosity of the fluid at high temperature) have been taken into account. Formation of streamers in transformer oil is mainly due to the field-dependent molecular ionization of hydrocarbon molecules at intense electric fields.¹ The field ionization is modeled using the Zener electron-tunneling function improved by Density Functional Theory (DFT).¹ Appropriate boundary conditions on electrode surfaces have also been assigned.^{1,5} The electric field intensity just close to the electrode surface is higher around the points with smaller radius of curvature which is particularly true for a needle electrode defined by the IEC 60897.⁶ This does not necessarily mean that the streamer breakdown occurs at lower voltages in a needle-needle gap rather than the needle-sphere electrode geometry. A sharp needle shape of the positive electrode assists the streamer initiation. However, if both electrodes are needles, the electric field in the middle of the gap will be relatively lower than what would be the case for the corresponding needle-sphere electrode geometry. This is caused by the fact that the

a) Author to whom correspondence should be addressed. Electronic mail: jouya@mit.edu

line integral of the electric field between electrodes is equal to the voltage drop across the electrodes. Since the voltage distributions across the two electrode configurations are different, and the electric field is extremely high in the vicinity of the needle electrode, it has to be lower in the halfway point between needle electrodes. The lower electric field in the region around the halfway point between two needle electrodes decreases the streamer acceleration, which consequently reduces the breakdown probability. Hence, the breakdown in the needle-needle electrode geometry occurs at higher voltages compared to the needle-sphere electrode geometry as shown in Fig. 1. The velocity of the streamers in different electrode geometries and gap distances can be derived from the streamer head trajectories along the shortest line which connects electrodes (on the axis of symmetry) as shown in Fig. 1. For the same applied voltages and gap distances, the average velocity is higher in the needle-sphere geometry. Specifically, the streamer velocity and acceleration toward the grounded sphere electrode increases earlier than in the needle-needle geometry. On the other hand, the maximum instantaneous velocity and acceleration of the streamer is higher when it propagates towards the grounded needle electrode. The trajectories of streamers in gaps ranging from 1 mm to 10 mm fit closely to polynomial and exponential functions for needle-sphere and needle-needle, respectively, as shown in Fig. 1.

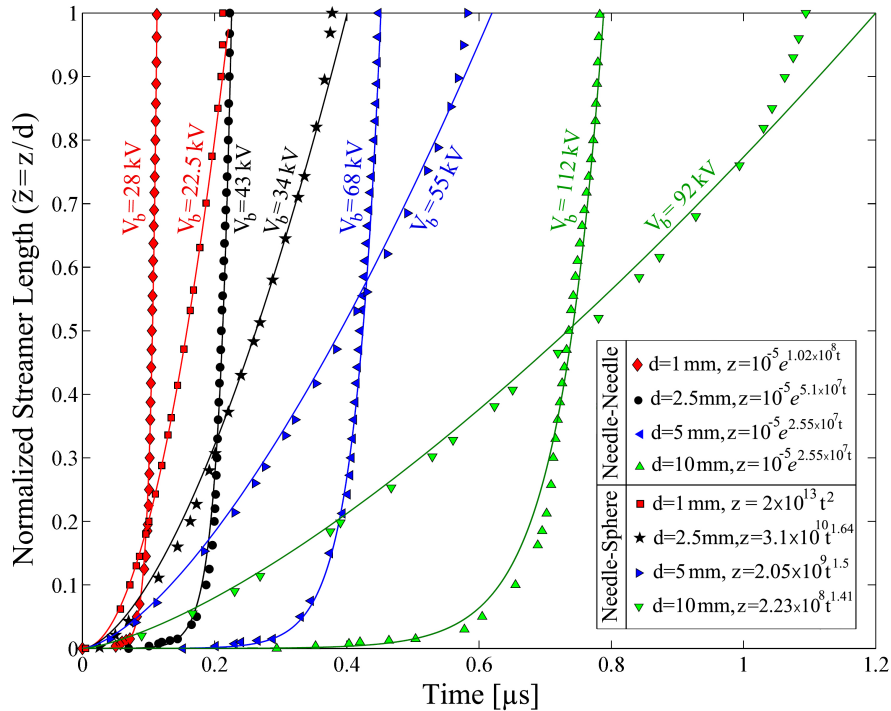


Fig. 1: Normalized length of the streamers for different electrode geometries and gap distances at breakdown voltages. Breakdown voltage is the minimum impulse voltage amplitude at which the streamer is able to reach the ground electrode and consequently breakdown occurs. The streamer lengths are fitted with exponential and single term polynomial curves for needle-needle and needle-sphere geometries respectively. Streamers require higher impulse voltages to reach the needle ground electrodes at any gap distance. The velocity of the streamer clearly increases when the streamer approaches the ground electrode at $z=d$.

Results show that the probability of breakdown will increase significantly if the applied impulse voltage is able to elongate the streamer within the last $\sim 10\%$ of the gap from the grounded sphere electrode and the last 20% of the gap from the grounded needle electrode. The reason is that the streamer acceleration respectively increases within the 10% and 20% of the gap distance from the grounded sphere and needle electrodes (as shown in Fig. 1).

Figure 2 shows the streamer head shape and position of the streamers emanating from a positive needle electrode until they reach the grounded sphere electrode (panels a, b, c, d) and the grounded needle electrode (panels e, f, g, h) for a 10 mm gap distance. The minimum applied voltage amplitude under which a streamer emanates from the positive needle (initiation voltage) is 11 kV for the needle-sphere and 17 kV for the needle-needle electrodes, 10 mm apart. Streamers formed by the initiation voltage do not necessarily reach the ground electrode, and therefore, do not lead to breakdown. If the applied voltage amplitude is greater than the initiation voltage but lower than the breakdown voltage, it creates streamers whose accelerations drop at some point (depending on the voltage amplitude) before it reaches the ground electrode. As soon as the streamer slows down the volume charge created by ionization along the streamer path starts to diffuse through the oil bulk. However, at voltages higher than breakdown voltage, the streamer eventually reaches the ground electrode as shown in Figs. 1 and 2.

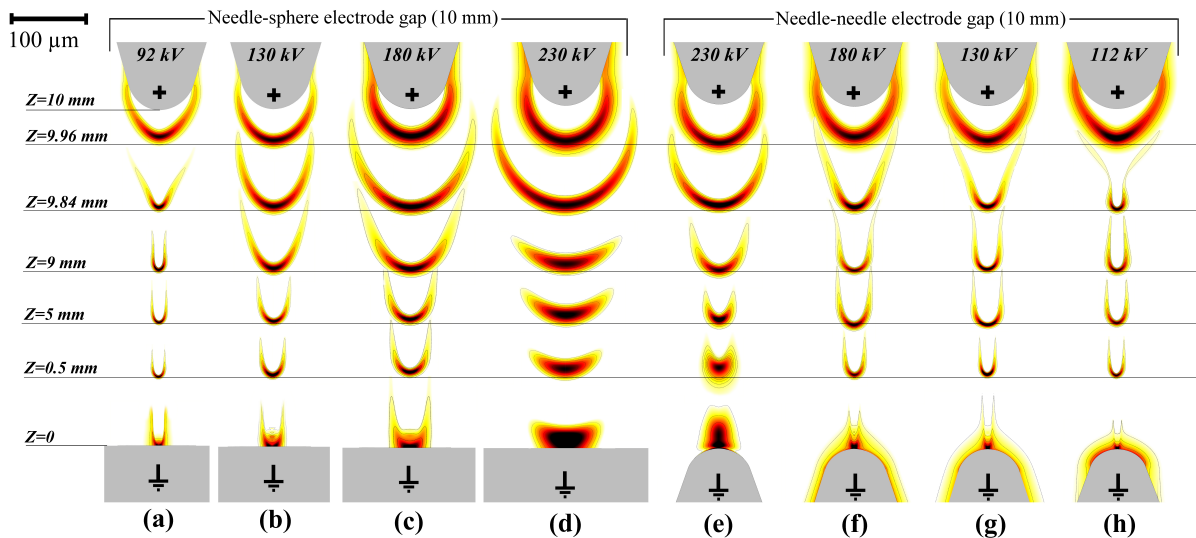


Fig. 2: Streamer breakdown in needle-sphere (a, b, c, d) and needle-needle (e, f, g, h) electrode gaps, 10 mm apart. Streamers always emanate from the positive needle and eventually hit the ground electrode. Electric field distributions are shown in the range of $0.5|E_{\max}|$ as the brightest color to $|E_{\max}|$ as the darkest color for positively applied impulse voltages with $0.1\mu\text{s}$ rise-time and different peak amplitudes. The values of $|E_{\max}|$ (for $0.1 < z < 9.9$ mm) and breakdown time are (a): 3.24 MV/cm, 1.092 μs ; (b): 3.06 MV/cm, 0.564 μs ; (c): 2.98 MV/cm, 0.328 μs ; (d): 2.56 MV/cm, 0.212 μs ; (e): 3.48 MV/cm, 0.098 μs ; (f): 3.47 MV/cm, 0.236 μs ; (g): 3.46 MV/cm, 0.483 μs ; (h): 3.48 MV/cm, 0.782 μs . The maximum electric field, $|E_{\max}|$, within 0.1 mm of electrodes is about 30% less. The trajectories of streamers are reasonably similar to Fig. 1 and can be approximately scaled by the applied voltage amplitude (considering the time to breakdown).

As can be seen in Fig. 2, the streamer column diameter and head radius of curvature are about 50% higher in the needle-sphere geometry than the needle-needle geometry. From the experimental point of view, it is difficult to visualize the streamer head position to find out when it hits the grounded electrode. Instead, it is much easier to measure the current passing through the electrodes,⁷ which can be considered as another good criteria of breakdown occurrence.⁷ Therefore, calculation of current passing through the gap greatly facilitates the validation process of the results. For this purpose, we integrate and add up the total fluxes of all charge carriers on the ground electrode surface, which gives the total current (conduction and displacement currents) to ground. Surely, the displacement component of the current is larger than conduction current before the streamer reaches the grounded electrode. However, after breakdown, the displacement current is relatively small compared to the conduction component.

To evaluate the displacement, the total surface charge on the grounded electrode, Q_s , is calculated over time, which is essentially equal to integral of perpendicular component of the displacement field on the surface, $\partial/\partial t (\int D_{\perp} ds)$. Therefore, it is enough to take the time derivative of Q_s to find the displacement current on the grounded electrode surface. Similarly, to calculate the conduction current, the total fluxes of all three carriers have to be algebraically summed up and integrated over the grounded electrode surface, i.e., $\int (\rho_p \mu_p E_{\perp} + \rho_e \mu_e E_{\perp} + \rho_n \mu_n E_{\perp}) ds$. Displacement and conduction currents at the grounded electrodes have been shown against time in Fig. 3 for both geometries.

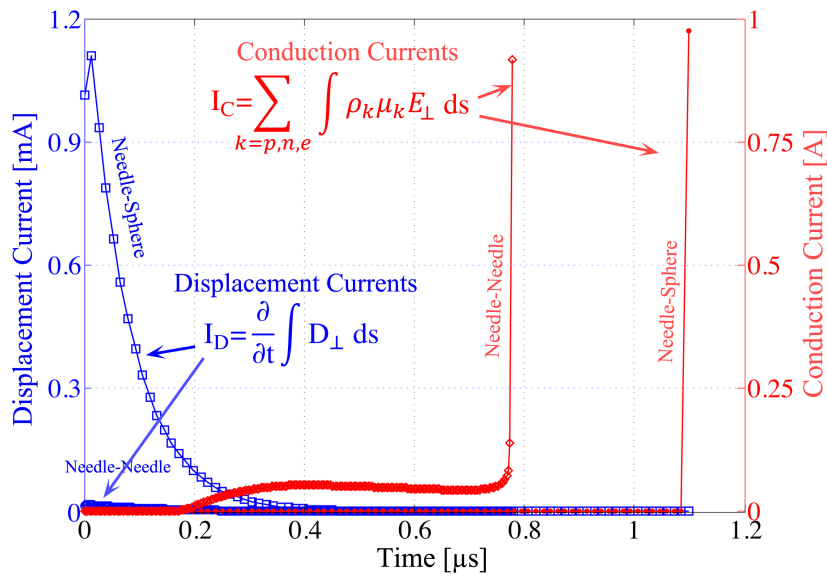


Fig. 3: Grounded electrodes' displacement and conduction currents, through needle-needle and needle-sphere electrodes 10 mm apart at their own breakdown voltages, i.e., 112 kV and 92 kV, respectively. The displacement current rises abruptly just after application of impulse voltage while conduction currents increases dramatically when the streamer hits the ground electrode at the times corresponding to $z/d=1$ in Fig. 1 (for $d=10$ mm). An initial rise in the conduction current of needle-needle geometry is due to the intense electric field in the vicinity of the grounded needle, which causes an appreciable ionization leading to a limited conduction current (~ 100 mA) until the streamer reaches the grounded needle.

Figure 4 shows the total current passing through the different gaps at breakdown voltages, which is the sum of displacement and conduction currents. The time variations of current in Fig. 4 correspond to the streamer trajectories shown in Fig. 1. As can be seen, the dramatic rise of breakdown current starts exactly at the instantaneous time that the streamer heads reaches the ground electrode. As a supporting evidence of breakdown, the current increases more than 10^8 fold in less than 30 ns for the needle-sphere electrode geometries and more than 10 fold in less than 20 ns for the needle-needle geometries.

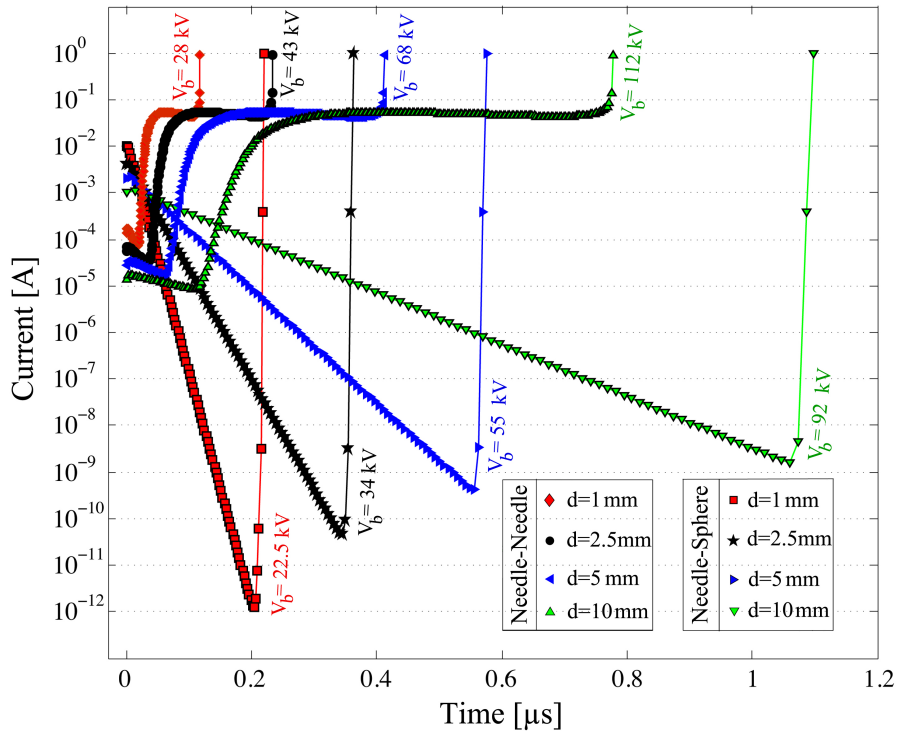


Fig. 4: Grounded electrodes' total current, conduction plus displacement, through different gaps and geometries at their own breakdown voltages. The current rises dramatically when the streamer hits the ground electrode at the times corresponding to $z/d=1$ in Fig. 1. Displacement current dominates the total current just after application of impulse voltage. Charge build up in the electrode gap capacitance attenuates this component, exponentially until the conduction current dominates the total current as the streamer reaches the grounded electrode which leads to breakdown (dramatic rise of current).

The model is no longer complete when the current rises beyond a few amperes, since due to high power dissipation along the streamer path, the streamer will be replaced by a high current arc, which requires additional physics such as plasma formation, thermal, impact and photo ionization and fluid convection to be modeled. Figure 5 shows the breakdown voltage for different gaps and electrode shapes.

The equations of charge conservation for electrons and different ions have been numerically solved using three well-known artificial streamline diffusions⁸: anisotropic, compensated streamline upwind Petrov-Galerkin and Galerkin least-square methods in combination with crosswind diffusion

artificial diffusion^{1,9}. Error-bars in Fig. 5 show the upper and lower bounds of the results obtained by each of the artificial streamline diffusions. The breakdown voltage is always higher when the streamer travels towards a needle ground electrode compared to sphere electrode for the same electrode gap distances. At similar applied impulse voltage peak amplitudes, the breakdown delay is slightly lower in the needle-sphere electrode geometry.

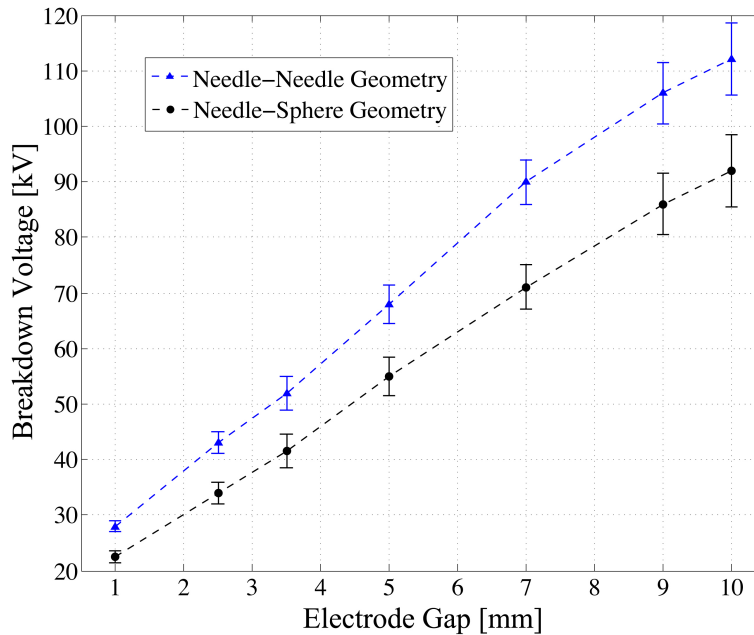


Fig. 5: Predicted breakdown voltage for different gap distances. Error-bars show the range of results obtained by each of the artificial streamline diffusions (anisotropic, compensated streamline upwind Petrov-Galerkin and Galerkin least-square methods) to solve the charge continuity equations.

This work has been supported by ABB Corporate Research (Västerås, Sweden), and IEEE Dielectrics and Electrical Insulation Society.

References:

- ¹ J. Jadidian, M. Zahn, N. Lavesson, O. Widlund, K. Borg, IEEE Trans. on Plasma Science, 40, 909, (2012).
- ² J. Jadidian, S. Mohseni, M. Jebeli Javan, E. Hashemi, A. A. Shayegani, K. Niayesh, IEEE Trans. on Plasma Science, 39, 2842, (2011).
- ³ J. Jadidian, IEEE Trans. on Plasma Science, 37, 1084, (2009).
- ⁴ J. Qian, R. P. Joshi, E. Schamiloglu, J. Gaudet, J. R. Woodworth, J. Lehr, J. Phys. D: Appl. Phys., 39, 359 (2006)
- ⁵ T. M. P. Briels, J. Kos, E. M. van Veldhuizen, U. Ebert, J. Phys. D: Appl. Phys., 39, 5201 (2006)

⁶ IEC Standard #60897, "Methods for the determination of the lightning impulse breakdown voltage of insulating liquids."

⁷ E. Kuffel, W. A. Zaengl, J. Kuffel, High Voltage Engineering: Fundamentals, Butterworth-Heinemann (2000)

⁸ Reference guide COMSOL Multiphysics 4.2a.

⁹ R. Codina, "A discontinuity-capturing cross-wind-dissipation for the finite element solution of the convection-diffusion equation," Computer Methods in Applied Mechanics and Eng., 110, 325 (1993)